Design strategies for viscoelastic damping treatment applied to automotive components

Etienne Balmès
SDTools and Ecole Centrale Paris/MSSMat balmes@sdtools.com
Sylvain Germès*
PSA Peugeot Citroën, Dpt. of Sciences for Automobiles and Advanced Research sylvain.germes@mpsa.com

SDTools has developed capabilities to analyze the response of structures with linear viscoelastic behavior. These software tools address material representation (in tabular or analytical forms), meshing of constrained viscoelastic treatments, placement strategies, and solvers for direct frequency response or eigenvalue solution of large problems. The paper discusses the proper constitution of FEM models of damped structures and methodologies that can be used to design damping treatments. Emphasis is put on describing design steps (placement, optimization, and validation) and approximation methods used during each phase. Illustrations are given on models of automotive components and performance of the NASTRAN, MATLAB, SDT software environment is discussed for vibroacoustic predictions of full vehicle body.

1 Introduction

Viscoelastic layer treatments have traditionally been considered as damping enhancement mechanisms. Such treatment work by having a significant fraction of strain energy transmitted through the viscoelastic material thus inducing energy dissipation in the form of heat.

Free layer treatments, illustrated in Figure 1, are widely used in the automotive industry as bitumen layers deposited on large sheet metal panels.[1] In the low frequency range, bending of the supporting plate induces an elongation of the surface of contact between the supporting metallic structure and the viscoelastic. This elongation is maximal near high curvature areas (beam center in the figure) where the viscoelastic works in traction/compression. To carry a significant load, the viscoelastic must thus be quite stiff which is usually not the case of very dissipative materials.

Constrained layer treatments are a first alternative allowing high dissipation with soft viscoelastic materials. By having a thin soft viscoelastic layer transmit shear loads between two stiff layers, one can induce very high shear levels and thus high dissipation. However, the localization of the dissipation has now moved to the edge of the layers. In such arrangement the shear stiffness of the viscoelastic must be high enough to transmit load from one stiff layer to the other. This load transfer mechanism makes the optimization of constrained layer treatments more difficult since boundary conditions and possible connections of the layers through weld spots have a strong influence.

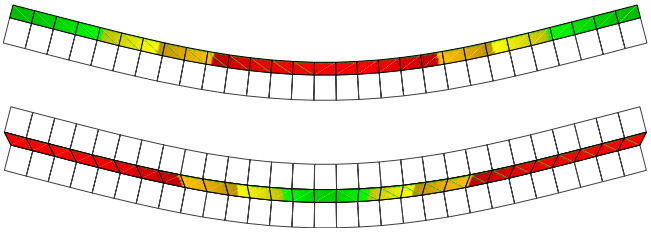

Fig. 1 Typical viscoelastic damping mechanims : free layer, constrained layer

These basic damping designs have in common a strong sensitivity to the actual localization of the treatment on a structure and to the relative properties of metallic and viscoelastic layers. The use of numerical simulations early in the design phase is thus critical to achieve good performance. This has motivated the developments detailed in this paper. Except from MSC/NASTRAN used as the reference FEM solver, software products used for this study have been developed by SDTools and validated through collaborations with EDF, PSA Peugeot-Citroen, ARTEC Aerospace and others.

Section 2 summarizes strategies used for modeling structures with viscoelastic materials. Points discussed include generation of sandwiches for curved surfaces, handling of surface offsets, need for mesh refinement, handling of mesh incompatibilities between underlying structure and placed treatment.

Section 3 describes a design cycle decomposed into placement, parametric optimization and final validations. The fact that efficiency in a layer treatment is governed by extension of the supporting surface is used in section 3.2 to motivate placement algorithms based on the study of surface strains of potential treatment areas. Once a design is placed and meshed, one must tune the damping properties. Viscoelastic treatments often have fairly narrow optima. Running a numerical

*Paper revised from IMAC 2004 Proceedings

optimization, as illustrated in section 3.3, is thus essential to achieve good performance. To finalize a design, predictions of poles, vibration, and acoustic response are made for a range of operating conditions in order to validate performance robustness. These steps are illustrated in section 3.4.

Finally, software architecture and current developments are discussed in the conclusion.

2 Issues with FEM modeling of viscoelastic treatments

Given a potential damping treatment topology, creating a FEM representation of the proposed treatment poses a number of questions: handling of surface offsets, generation of sandwiches for curved surfaces, need for mesh refinement, handling of mesh incompatibilities between underlying structure and a given treatment.

2.1 Meshing sandwich structures

Two main strategies have been considered to model sandwich structures: building higher order shell models[2] or connecting multiple elements. The main problem with the higher order element approach is that developing good shell elements is very difficult so that most developments for sandwiches will not perform as well as state of the art shell elements. The multiple element strategy is also the only available for immediate implementation into industrial FEM software.

To properly account for shear effects in the viscoelastic layer, the offsets between the neutral fiber and the shell surface are most of the time essential. Rather than defining offsets for shell elements,[3] rigid links between the shell nodes and the volume element are used here as shown in figure 2. Although this generates additional nodes (4 node layers for a single constrained layer model), this strategy accommodates all possible layer configurations. During resolution, the model is smaller since all viscoelastic volume nodes are constrained.

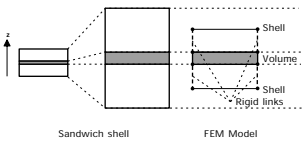

Fig. 2 Shell/volume/shell model for sandwiches

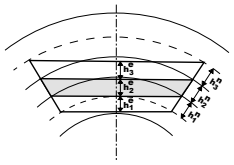

Fig. 3 Problems with thickness definitions in shells with significant curvature

For stiff layers, shells are preferred over volumes, because volume element formulations are sensitive to shear locking when considering high aspect ratio (dimensions of the element large compared to thickness).

For soft layers, the use of a volume element both necessary, because shell elements will typically not correctly represent high shear through the thickness, and acceptable, because almost all their energy is associated with shear so that they will not lock in bending.[4] Note that shear corrections used in some FEM codes to allow bending representation with volumes must be turned off to obtain appropriate results. Finally there are doubts on how to properly model the through the layer compression stiffness of a very thin viscoelastic layer (this can have significant effects on curved layers).

Automated layer mesh generation from a selected area of a nominal shell model is a basic need. Figure 3 illustrates the fact that for curved shells, the use of flat elements generates a distinction between layer thicknesses along the element normal h_i^e or along the normal at nodes h_i^n. This distinction is important for relatively coarse meshes of press formed parts (as the floor panel of figure 8). While the solution retained here is to preserve thickness values along normal at nodes, the range of validity of this approach is unclear.

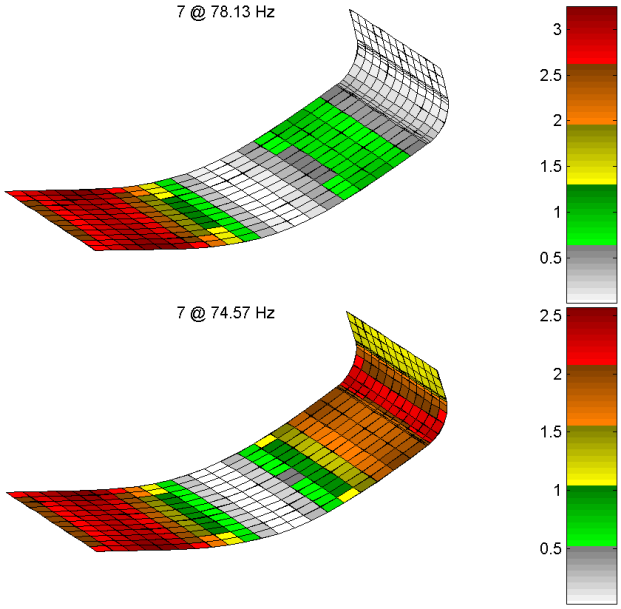

Fig. 4 Energy density in the viscoelastic layer of a simple folded sandwich plate. (Top) High stiffness viscoelastic in the fold. (Bottom) equal stiffness in the fold and elsewhere.

For press formed sandwiches, there are further unknowns in how the forming process affects the core thickness and material properties. In particular, most materials used for their high damping properties are also very sensitive to static pre-stress.

For a simple folded plate, figure 4 illustrates how the modal frequencies and energy distribution in the viscoelastic layer are modified if the shear modulus is multiplied by 10 in the fold. Such behavior was found in tests and motivated the study in Ref.,[5] where the effect of static pre-stress is measured experimentally. Overall, predicting the effects press forming or folding

sandwiches is still a very open issue.

A final difficulty is to deal properly with boundary conditions of the skin layers. Since differential motion of the skins plays a major role in the effectiveness of the core, the boundary conditions of each layer has to be considered separately. This is easily illustrated by the generation of cuts in constraining layers.[6,3]

2.2 Mesh convergence and non conformity

As illustrated in figure 1 the dissipation if often localized on a fairly small sub-part of the structure. It is thus quite important to validate the accuracy of predictions obtained with various mesh refinements. Figure 5 illustrates a convergence study where a constrained layer damping treatment is refined and one compares the strain energy density maps for two levels of refinement. The strain energy maps, clearly indicate edge effects, which are typical of constrained layer treatments. In such studies the author's have usually found, that the distribution of constraints is well predicted and energy fractions (strain energy in the viscoelastic compared to total strain energy in the model) predicted with the fine and coarse meshes do not show significant differences.

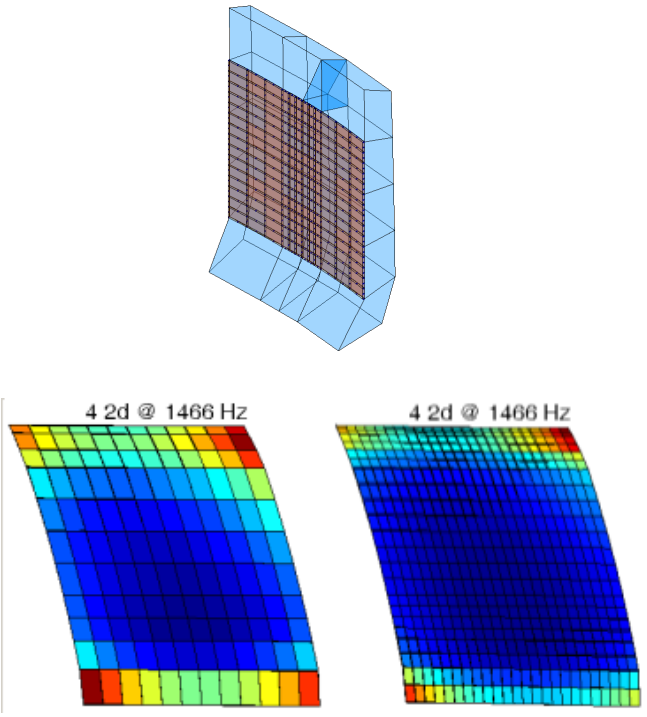

Fig. 5 Zoom on the refined mesh of a constrained layer damping treatment placed on a volume model. Comparisons of strain energy maps for two levels of refinement.

When considering free placement of damping devices (see section 3.2), one is rapidly faced with the problem of incompatible meshes. For discrete connections, where loads are transmitted at isolated points with at most one point on a given element of the supporting structure, the problem is very much related to that of the representation of weld spots.

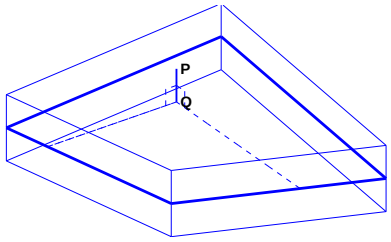

Fig. 6 Non conform mesh handling

The solution retained here is to first project the arbitrarily located connection point P on the element surface onto a point Q on the neutral fiber used where element nodes are located. Then $Q1$ or $P1$ shape functions and their derivatives are used to define a linear relation between the 6 degree of freedom of point Q and the 3 or 4 nodes of the facing surface. Motion at P is then deduced using a linearized rigid PQ link. One chooses to ignore rotations at the nodes since their use is very dependent on the shell element formulation.

2.3 Handling viscoelastic materials

The basic assumption of linear viscoelasticity is the existence of a relaxation function $h(t)$ such that the stress is obtained as a convolution with the strain history. Using the Laplace transform, one obtains an equivalent representation where the material is now characterized by the *Complex Modulus* E (transform of the relaxation function)

$$\sigma(s) = E(s, T, \epsilon_0)\varepsilon(s) = (E' + iE'')\varepsilon(s) \qquad (1)$$

For all practical purposes, one can thus, in the frequency domain, deal with viscoelasticity as a special case of elasticity where the material properties are complex and depend on frequency, temperature, initial deformation and other environmental factors.

Dependence on environmental factors should *a priori* be arbitrary. In practice however, one assumes, and generally verifies, that environmental factors only act as shifts on the frequency[7] (this is the so called *temperature/frequency equivalence principle*). Tests thus seek to characterize a master curve $E_m(s)$ and a shift function $\alpha(T, \epsilon_0)$ describing the modulus as

$$E(s, T, \epsilon_0) = E_m(\alpha(T, \epsilon_0)s) \qquad (2)$$

For simulations, a function generating E for all values of s, T, ϵ_0 must be created. As illustrated in figure 7, this function must handle continuations outside of the range of the experimental nomogram, since these are likely to happen in a design study. Useful complements are the ability to generate nomograms (these are standard representations of frequency and temperature dependencies in a single plot[7]), to combine

experimental material characterizations into a nomogram, or to estimate the parameters of an analytic representation of a test.

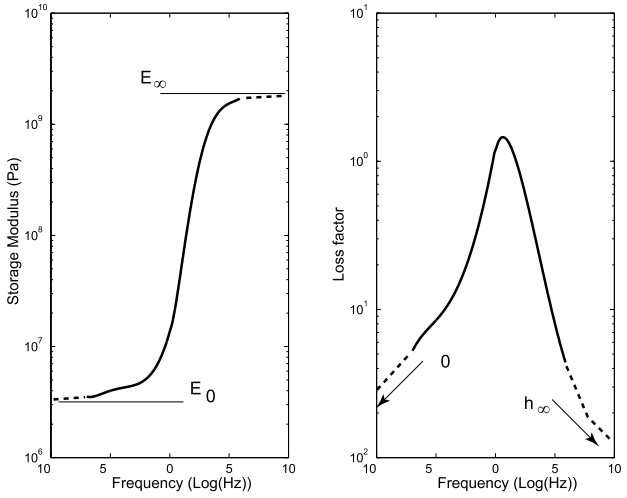

Fig. 7 Master curve of a real material

When proper care is taken, both analytical and tabular representations of $E(s)$ are capable of closely approximating material test data. They thus have the same "physical" validity. The differences are really seen in how each representation can be integrated in FEM solvers and in the validity of extrapolations outside the tested material behavior range. On the later point, the actual process used to obtain the parameters has a strong influence, it may thus be easier to obtain a good model with a particular representation even if that representation is not inherently better.

While rational fractions or fractional derivatives[8] are analytical representation of particular interest to implement constant matrix solvers,[9,10,11,12,13] it was found that all design and validation phases can be handled properly using representations where $E(i\omega)$ is interpolated from tabulated material test data. This is thus the solution retained here.

2.4 Practical solvers for damped vibroacoustic problems

Given a constitutive law described by parameters $E_i(s,T,\epsilon_0)$, one can use the fact that element stiffness matrices depend linearly on those parameters to build a representation of the dynamic stiffness as a linear combination of constant matrices

$$[Z(E_i,s)] = \left[Ms^2 + K_e + \sum_i E_i(s,T,\epsilon_0)\frac{K_{vi}(E_0)}{E_0} \right] \quad (3)$$

This representation is the basis used to develop practical solvers for viscoelastic vibration problems.

Typically, the final predictions of interest are responses at target locations to loads applied on the structure. Assuming that the responses are linearly related to model DOFs by the observation matrix $[c]$, and loads can be decomposed into input shapes $[b]$ and time/frequency dependent inputs $\{u(s)\}$, one must compute

$$\begin{array}{rcl} [Z(E_i,s)]\{q\} & = & [b]\{u(\omega)\} \\ \{y(\omega)\} & = & [c]\{q\} \end{array} \quad (4)$$

at various operating points (values of frequency s, temperature T and/or pre-stress ϵ_0, leading to E_i values).

While most FEM software will handle one instance of problem (4) easily, typical design studies require computation of a few thousand frequency points at tens of design points thus making direct frequency resolution totally impractical.

Fixed basis model reduction builds a fixed approximation subspace T and estimates the response using a standard Ritz-Galerkin approximation

$$\{\hat{q}(\omega)\} \approx [T]\left[T^T Z(\omega,T,\epsilon_0)T\right]^{-1}\left[T^T\right]\{F(\omega)\}, \quad (5)$$

Starting with a tangent elastic stiffness $K_0 = Re\left(Z(E_i,0)\right)$, reduction bases that are used classically are

- normal (real) modes of the structure

$$T = [\phi_{1:NM}(K_0)], \quad (6)$$

  on can consider modes of a structure with a nominal treatment or modes of the untreated structure and estimate response in the treatment by static condensation.

- normal (real) modes of the structure with static correction for the viscoelastic loads generated by these shapes[14]

$$T = \left[\phi_{1:NM}(K_0) \;\; K_0^{-1}\mathrm{Im}(Z(\omega_0,E_{i0}))\phi_j\right], \quad (7)$$

- higher order bases resulting from the Residual Iteration process described in .[15]

Each of these approximations is used successively in the design process. Nominal modes (6) for placement (section 3.2), the first order correction (7) for parametric optimization (section 3.3) and higher order iterative solutions for the final validations (section 3.4).

2.5 Extensions for vibroacoustic predictions

In many practical cases, the final prediction of interest is a vibroacoustic response where the structure is coupled with a compressible non-weighing fluid, with or without a free surface. Using a finite element formulation for this type of problem, leads[16] to equations of the form

$$\left[\begin{bmatrix} M & 0 \\ C^T & K_p \end{bmatrix} s^2 + \begin{bmatrix} K(s) & -C \\ 0 & F \end{bmatrix}\right]\begin{Bmatrix} q \\ p \end{Bmatrix} = \begin{Bmatrix} F^{ex} \\ 0 \end{Bmatrix} \quad (8)$$

with q the displacements of the structure, p the pressure variations in the fluid and F^{ex} the external load applied to the structure.

Given a reduction basis T_s for the structure, one builds a reduction basis containing fluid modes within the bandwidth of interest and static corrections for the effects of vectors in T_s. Thus the resulting basis for the fluid model is

$$[T_f] = \left[\phi_{f,1:NM} \quad [F]^{-1}[C]^T[T_s]\right] \tag{9}$$

Similar equations can of course be developped for applications where the fluid is represented using boundary elements.[17]

3 Design and validation phases

3.1 Outline of the design process

The vibration damping design methodology considered here starts with an elastic model of the structure. A first understanding of the dynamic performance is obtained by computing modes and frequency responses using classical damping models

- modal damping : where a viscous damping ratio is associated with each mode of the elastic model. These damping ratio are either arbitrary (1 % for all modes, etc.) or derived from experimental tests of a prototype structure.
- hysteretic damping : where a constant loss factor is associated with each material in the model. This is equivalent to selecting one target frequency in the master curve shown in figure 7.

The objective of this first analysis is to select a set of target modes that one whishes to damp. Given these elastic modes, the design of a damping treatment is decomposed in three phases that will be illustrated in the following sections.

One first places treatments in potentially beneficial locations. The strategy retained is to base this placement on particular properties of the target modes. The objective functions used are strain energy fractions or levels of membrane strain on surfaces.

In a second phase, one seeks an optimum for the characteristic stiffness k_v of the viscoelastic layer. For a typical mechanism where the layer works in shear, one has $k_v = G\ S_v/e_v$ where the modulus G can be selected in a wide range of viscoelastic materials and the treated surface S_v and layer thickness e_v are also fairly arbitrary. This second phase is key to find a parametric optimum where damping is really high. The considered objective functions are strain energy fractions in the viscoelastic material and estimates of damping levels for constant complex moduli.

During the final validation phase, one selects acceptable damping materials and performs robustness evaluations using a realistic representation of the temperature and frequency dependence of their properties. The objective functions are then complex modes and selected frequency response spectra.

3.2 Placement of viscoelastic treatments

A number of placement algorithms are based extensive searches within a fixed number of potential locations.[18,19] These strategies are however very costly because they have to test many configurations to retain just a few. Strategies that gradually build the treatment, although potentially sub-optimal, are much more affordable computationally.

As detailed in the introduction, viscoelastic damping treatments for bending surfaces are efficient because a fiber away from the neutral axis elongates when the surface bends. This elongation can be quantified using membrane strains on the actual free surface (rather than the element node plane).

Figure 8 shows the surface membrane strain energy density averaged over the first 50 modes of an automotive floor panel.[20] This map clearly indicates high potential areas between the two embossing of the rear half and near most of the high curvature areas generated during the press forming of the floor panel. It is quite important to note that membrane strains, and thus such maps, are very different on the shell neutral axis or the free surfaces. Another result is that placing free or constrained layer treatments on the flat parts of the panel is not an optimal strategy.

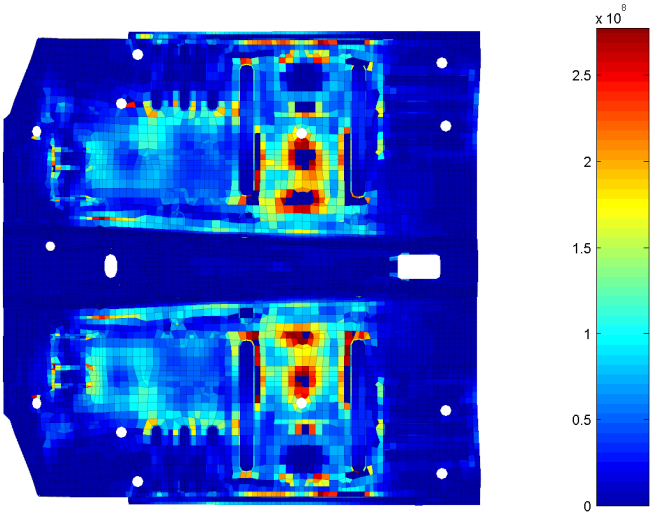

Fig. 8 Strain energy density estimated on the surface of an automotive floor panel. Frequency weighted average for the first 50 modes.

Surface strain maps have also been successfully used to place directional damping treatments using the fact that the principal strain directions provide an optimal orientation.

3.3 Parametric optimization during design phases

Given a placement result, one finds that damping levels have extremely significant variations in the range of possible layer thickness and viscoelastic moduli. Optimizing layer properties is thus a key step to achieve interesting performance.

An exact study of the influence of thickness variations is an enormous task since it implies remeshing of the layers and full solution of the frequency response and/or modes. To get a first cut at the task, one linearizes the influence of thickness on the element matrices.

Shear stiffness being inversely proportional to thickness, one can approximate the stiffness contribution of a layer working in shear for a range of thickness using

$$K_{vi}(h_v, E_i) \approx \frac{h_{v0}}{h_v} \frac{E_i(s,T,\epsilon_0)}{E_0} K_{vi}(E_0) \qquad (10)$$

For layers working in extension (typically constraining layers that are not too thick), the energy is proportional to thickness. One thus has, for an elastic constraining layer

$$K_{ci}(h_c) \approx \frac{h_c}{h_{c0}} K_{ci}(E_i) \qquad (11)$$

Based on these approximations, one computes the evolution of poles and FRFs with thickness.

In simple cases where a few modes are of interest, it is usually easier to use pole tracking to determine the optimal set of parameters. For the floor pannel of figure 8 (ref.[20]), figure 9 shows the evolution of the damping of 4 poles as a function of layer thickness for patch configuration B1, material TA at 20^oC (nominal viscoelastic layer at $h_{v0} = 50\mu m$ and constraining at $h_{c0} = .3mm$). This map indicates that dissipation could be augmented by increasing h_c to .5 or $.7mm$. For h_v the $50\mu m$ nominal seems reasonable but the optimum differs for each pole (and the reliability of pole estimates at higher frequencies can be questioned).

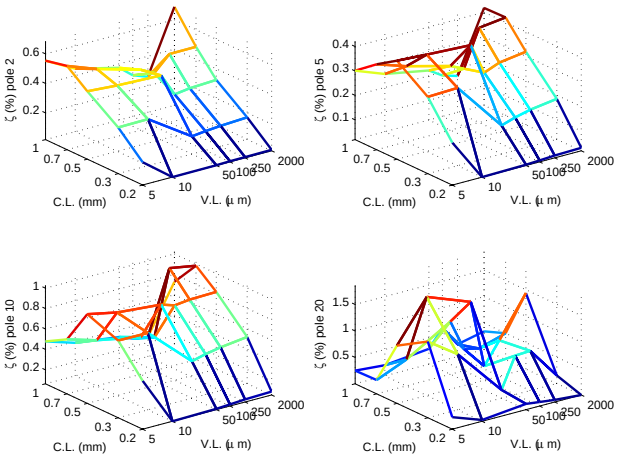

Fig. 9 Influence of layer thickness on the damping ratio of pole 1.

In reality, the objective of interest is the frequency response in the 10-200 Hz range which contains 75 modes. As shown in,[20] a direct exploitation of the responses computed for this range of layer thickness is difficult. The retained objective function is thus the

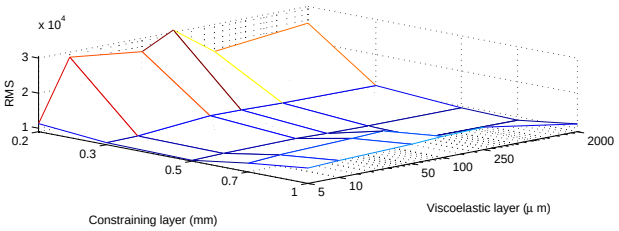

Fig. 10 Influence of layer thickness on the RMS acceleration for range 10-200 Hz.

RMS response of load to acceleration transfer functions.

The map of RMS responses in figure 10 confirms the need to increase the constraining layer thickness (to .5mm). For the viscoelastic layer thickness the variations are quite low which confirms the pole tracking indications.

3.4 Final design and validation phases

Once a design is stabilized, one must validate the accuracy of the approximate predictions obtained in the design phase and make decisions on a number of practical issues.

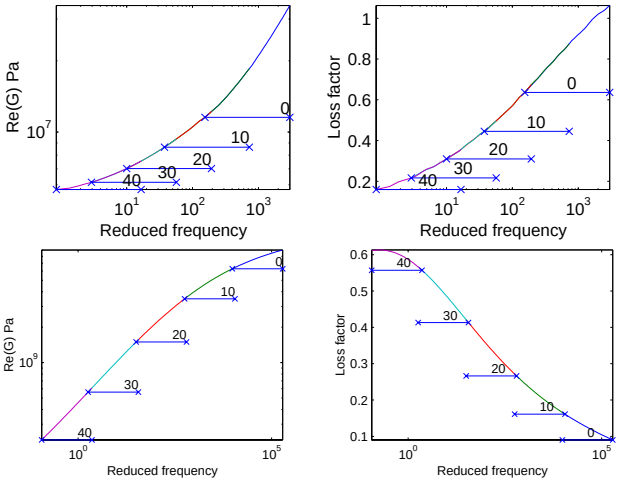

Fig. 11 Nomogram of SM50e and PL3023 with 10-200 Hz frequency bands at various temperatures.

When selecting a material to be used in a viscoelastic damping treatment, it is essential to understand how the material behaves in the temperature/frequency range of interest. Before actually defining a geometry, one can display reduced frequency bands on the master modulus curve. For example, figure 11 illustrates that material SM50e has low stiffness and loss factor for low frequency (10-200 Hz) near room temperature operation. The same material would be efficient for sub-zero temperatures or a higher frequency band (5-20 kHz).

For the much stiffer PL3023, considered for free layer damping designs in Ref.,[20] the operating range of interest is above loss factor peak, so that reducing temperature will actually decrease damping. The smaller band overlap also illustrates a higher sensitivity to operating conditions.

An important validation is the robustness to temperature variations. This is done by computing FRFs for a frequency/temperature range as shown in figure 12. While an improvement can be noticed around 20^oC the damping here is quite low and the plot is thus difficult to interpret. RMS plots are better indicators of performance in this context.

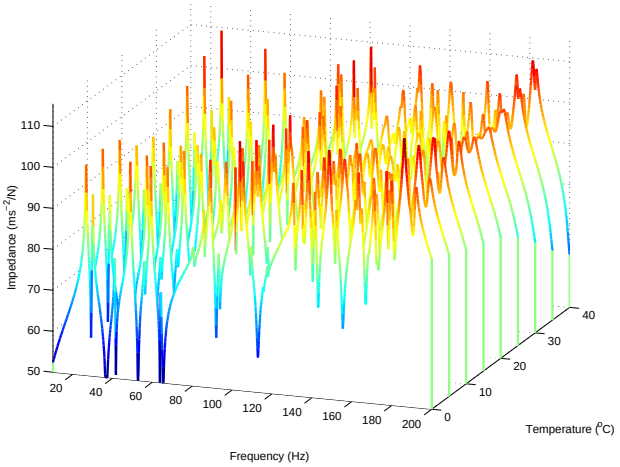

Fig. 12 FRFs for a frequency/temperature range (Floor panel case B1/Ta).

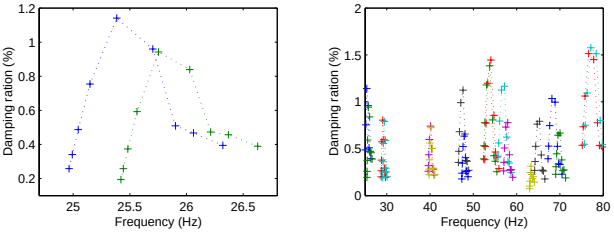

Fig. 13 Pole tracking on the 0+40^oC range (Floor panel, case B1/Ta)

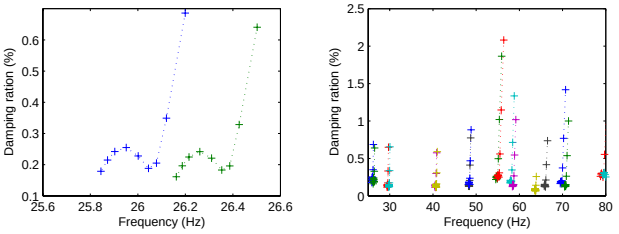

Fig. 14 Pole tracking on the -40+40^oC range (Floor panel, case B1/SM50e[20])

Pole tracking as shown in figure 13 is a useful alternative. For the considered case it confirms that indeed optimal damping is achieved near 20^oC.

Care must however be taken in using fixed basis reduced models over a wide parametric range. Figure 14 for example shows the classical temperature optimum (very similar to that of figure 13) but also a strong increase of damping at very low temperatures. This effect disappears when changing the tangent elastic stiffness $K_0 = Re\,(Z(E_i, 0))$ to reflect a much higher nominal value of the viscoelastic layer. Indicators to warn of likely result inaccuracy are thus needed as intermediates between design and verification solvers.

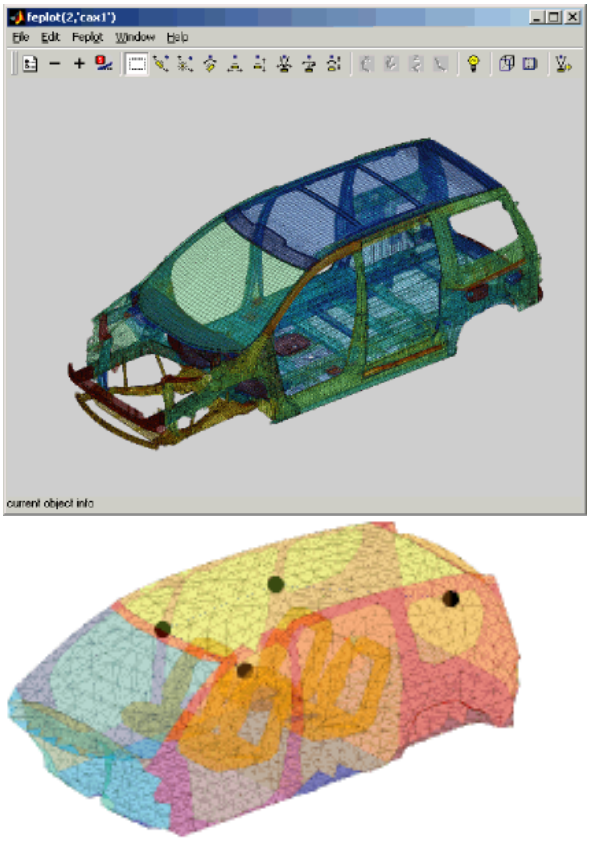

Fig. 15 Solid model of the C8 body and fluid model of it's interior cavity.

In automotive applications, validations will often include vibroacoustic predictions. Figure 15 shows the models of a Citroen C8 body. The solid model uses approximately 1e6 DOFs, 200 000 Nodes and elements, 100 000 linear constraints. The fluid model contains 2400 nodes and 10 000 elements. Since the solid model is not closed, openings in the body are assumed infinitely rigid.

The target transfers are from load applied on two engine mounts to four locations representative of passenger ear locations. 304 for structural modes up to 225 Hz are retained for frequency response predictions. Figure 16 shows a typical study of interest, where one compares acoustic levels for configurations without and with windshield damping.

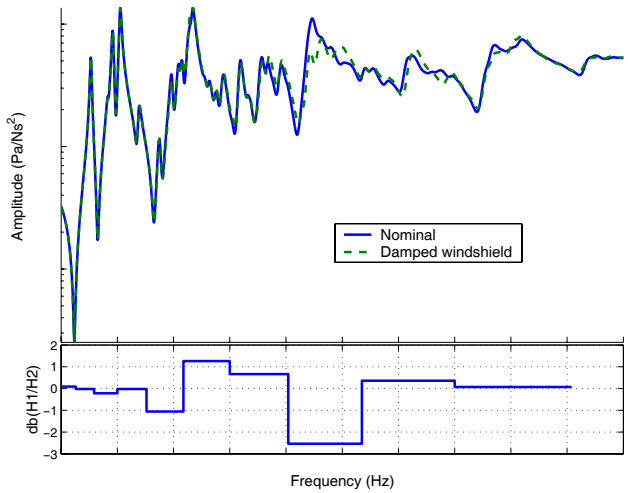

Fig. 16 Effect of windshield damping on the vibroacoustic response of automotive body.

4 Conclusion

The results presented here are obtained using a number software packages.

- *MSC/NASTRAN* is used to generate the initial FEM solution. This is necessary because these solutions are the reference undamped models in use many industries. Similarly *ANSYS* can be used as reference.

- *FEMLink* is used to import *NASTRAN* results into the *MATLAB/SDT* environment and export additional elements for the damping treatments for inclusion in the reference *NASTRAN* model. Such export is needed to allow reuse of designs generated in the by the specific tools listed below.

- The *SDT* (Structural Dynamics Toolbox) is used as the computational and visualization engine for all placement and validation phases. Its open architecture and extremely flexible programming environment was critical in allowing rapid testing of many strategies. Its model reduction tools are also used extensively.

- The *Viscoelatic Vibration Toolbox* groups all the analysis methods developed by SDTools for expert studies in the vibroacoustic response of damped structures. These include sandwich generation methods, nomogram handling tools and a database of existing materials, solvers for direct frequency response and pole tracking, tools for vibroacoustic predictions.

The overall objective of the developments detailed here are to provide advanced design tools. Having a flexible development environment that allows rapid software prototyping is thus a key constraint that motivated the choice of MATLAB (for programming) and SDT for the FEM architecture.

One main difficulty is to obtain the reduction basis and reduced matrices associated to the dynamic stiffness (3). MATLAB is a 32 bit application that in practice cannot allocate more than 1.5 GB for variables. The 304 vectors of the C8 model require 2.4 GB memory. The model reduction steps described in section 2 thus require out-of-core operations which are available in NASTRAN, but require difficult DMAP programming, and are just being developed for SDT. Thus in practice, one is currently capable of generating all reduced model forms when the basis size is below 500 MB.

Once a reduced parameterized model is created, generation of the coupled equations for a vibroacoustic problem and parametric studies for optimization and/or validation can easily be performed within MATLAB/SDT. For the C8 vibroacoustic response, computing 2048 frequency points only takes a couple minutes. Extensive design studies can thus be performed when they would be impractical if a NASTRAN batch job needed to be submitted every time.

For vibroacoustic predictions in the automotive industry, global performance is currently estimated using crude damping models (constant loss factors at best). The strategies illustrated here were thus introduced to allow realistic predictions of the effects of damping materials, thus leading to better designs.

While many applications were shown, this paper really describes work in progress. The main conclusion is that the proposed design process can be applied for practical automotive applications.

Areas of active development by *SDTools* are

- placement strategies for classical constrained layers or other damping devices such as SPADD from Artec Aerospace;[21]

- software optimization for large models, optimization phases, and vibroacoustic predictions;

- development of initial design tools packaged for use by non experts.

References

[1]**Bienert, J.**, *Optimisation of Damping Layers in Car Bodies*, ISMA, pp. 2005–2010, 2002.

[2]**Kant, T.** and **Swaminthan, K.**, *Free vibration of isotropic, orthotropic and multilayer plates based on higher order refined theories*, Journal of Sound and Vibration, Vol. 241, No. 2, pp. 319–327, 2001.

[3]**Balmès, E.** and **Bobillot, A.**, *Analysis and Design Tools for Structures Damped by Viscoelastic Materials*, International Modal Analysis Conference, February 2002.

[4]**Plouin, A.** and **Balmès, E.**, *A test validated model of plates with constrained viscoelastic materials*, International Modal Analysis Conference, pp. 194–200, 1999.

[5]**Kergourlay, G.**, Mesure et prédiction de structures viscoélastiques - Application à une enceinte acoustique, Ph.D. thesis, Ecole Centrale de Paris, 2004.

[6]**Mead, D.** and **Markus, S.**, *The Forced Vibration of a Three Layer, Damped Sandwich Beam with Arbitrary Boundary Conditions*, Journal of Sound and Vibration, Vol. 10, No. 2, pp. 163–175, 1969.

[7]**Nashif, A., Jones, D.** and **Henderson, J.**, Vibration Damping, John Wiley and Sons, 1985.

[8]**Blakely, K.**, MSC/NASTRAN v68, Basic Dynamic Analysis, MacNeal Shwendler Corp., Los Angeles, CA, December,, 1993.

[9]**Golla, D.** and **Hughes, P.**, *Dynamics of viscoelastic structures – A time domain finite element formulation*, Journal of Applied Mechanics, Vol. 52, pp. 897–906, 1985.

[10]**McTavish, D.** and **Hugues, P.**, *Finite Element Modeling of Linear Viscoelastic Structures*, ASME Biennal Conference on Mechanical Vibration and Noise, sep 1987.

[11]**Lesieutre, G.** and **Bianchini, E.**, *Time Domain Modeling of Linear Viscoelasticity Using Augmenting Thermodynamic Fields*, SDM Conference, AIAA paper 93-1550-CP, pp. 2101–2109, 1993.

[12]**Bianchini, E.** and **Lesieutre, G.**, *Viscoelastic constrained-layer damping - Time domain finite element modeling and experimental results*, SDM Conference, AIAA paper 94-1652-CP, pp. 2666–2676, 1994.

[13]**Lesieutre, G.** and **Bianchini, E.**, *Time Domain Modeling of Linear Viscoelasticity Using Augmenting Thermodynamic Fields*, J. Vibration and Acoustics, Vol. 117, pp. 424–430, 1995.

[14]**Plouin, A.** and **Balmès, E.**, *Steel/viscoelastic/steel sandwich shells. Computational methods and experimental validations.*, International Modal Analysis Conference, pp. 384–390, 2000.

[15]**Bobillot, A.**, Méthodes de réduction pour le recalage. Application au cas d'Ariane 5, Ph.D. thesis, Ecole Centrale de Paris, 2002.

[16]**Morand, H. J.-P.** and **Ohayon, R.**, Fluid Structure Interaction, J. Wiley & Sons 1995, Masson 1992.

[17]**Kergourlay, G., Balmès, E.** and **Clouteau, D.**, *Interface model reduction for efficient FEM/BEM coupling*, International Seminar on Modal Analysis, Leuven, September 2000.

[18]**Anderson, E.**, Actuator Placement for Structural Control, MIT PhD thesis, 1993.

[19]**Bandini, M., Governi, L.** and **Pierini, M.**, *Optimal design of damping material distribution in dynamically excited panels*, ISMA, pp. 441–449, 2002.

[20]**Balmès, E.** and **Germès, S.**, *Tools for Viscoelastic Damping Treatment Design. Application to an Automotive Floor Panel.*, ISMA, September 2002.

[21]**Balmès, E.**, *Tools for Viscoelastic Damping Treatment Design. Application to an Automotive Floor Panel.*, ISMA, September 2004.